

## Elimination of the degenerate trajectory of a single atom strongly coupled to a tilted TEM<sub>10</sub> cavity mode

Pengfei Zhang, Yanqiang Guo, Zhuoheng Li, Yuchi Zhang,<sup>\*</sup> Yanfeng Zhang, Jinjin Du, Gang Li, Junmin Wang, and Tiancai Zhang<sup>†</sup>

*State Key Laboratory of Quantum Optics and Quantum Optics Devices, Institute of Opto-Electronics, Shanxi University, Taiyuan 030006, China*

(Received 9 December 2010; published 28 March 2011)

We demonstrate the trajectory measurement of the single neutral atoms deterministically using a high-finesse optical microcavity. The single atom strongly couples to the high-order transverse vacuum TEM<sub>10</sub> mode, instead of the usual TEM<sub>00</sub> mode, and the parameters of the system are  $(g_{10}, \kappa, \gamma) = 2\pi \times (20.5, 2.6, 2.6)$  MHz. The atoms simply fall down freely from the magneto-optical trap into the cavity modes, and the trajectories of the single atoms are linear. The transmission spectra of atoms passing through the TEM<sub>10</sub> mode are detected by single-photon counting modules and are well fitted. Thanks to the tilted cavity transverse TEM<sub>10</sub> mode, which is inclined to the vertical direction  $\sim 45^\circ$ , it helps us to eliminate the degenerate trajectory of the single atom falling through the cavity and to obtain a unique atom trajectory. An atom position with a high precision of  $0.1 \mu\text{m}$  in the off-axis direction (axis  $y$ ) is obtained, and a spatial resolution of  $5.6 \mu\text{m}$  is achieved in a time interval of  $10 \mu\text{s}$  along the vertical direction (axis  $x$ ). The average velocity of the atoms is also measured from the atom transits, which determines independently the temperature of the atoms in a magneto-optical trap,  $186 \pm 19 \mu\text{K}$ .

DOI: [10.1103/PhysRevA.83.031804](https://doi.org/10.1103/PhysRevA.83.031804)

PACS number(s): 42.50.Pq, 37.30.+i, 37.10.Jk

Manipulation of neutral single atoms known as a basic system of quantum optics and atomic physics for the last two decades, either in free space [1–6] or inside a cavity [7–10]. From the early hot and stochastic atom beam to the cold and deterministic control of individual atoms, the single atom is now a good system to demonstrate the quantum logic gate [11] and the quantum register [4,12]. In order to get information from a single atom, two predominant methods are used in most experiments. One is to detect directly the fluorescence of the atoms using a specially designed light collection system and a high-efficiency optical detector; another is to detect the transmitted light from a high-finesse optical cavity, which is usually strongly coupled to the atoms [13]. The cavity quantum electrodynamics (CQED) system has been used to detect single atoms as well as the atom trajectory [14]. A large coupling between the single atom and the cavity provides the capability of measuring the atom trajectory through the transmission of the cavity [15,16]. Moreover, atomic position tracking is interesting because of its close connection to cavity cooling [10] and optomechanics [17].

In the earlier experiments, an atom beam has been used in CQED experiments [18–20] and the duration of the atom transits was so short that the detection of individual atom positions and their trajectories could not be accomplished in real time. The development of the cold atom technology and the manipulation of single atoms [21,22] provide the effective tools for CQED experiments. Either through the atom free falling down or launching up to the cavity, the transit time of atoms in the cavity mode lasted more than  $100 \mu\text{s}$  [15,16], and the trajectories of the single atom can be measured. In 2000, Hood *et al.* trapped a single atom inside a microcavity for milliseconds, and the two-dimensional (2D) atom trajectories

in the plane perpendicular to the cavity axis were reconstructed from the cavity transmissions, and they obtained  $\sim 2 \mu\text{m}$  of the spatial resolution in a  $10\text{-}\mu\text{s}$  time interval [14]. However, for all these experiments mentioned above, the atom was coupled to the fundamental Hermite-Gaussian TEM<sub>00</sub> mode. Although the coupling between the atom and cavity TEM<sub>00</sub> mode is stronger than all the other modes when the atom passes in the center of the cavity mode, the displacements of the atom along the cavity axis, or between a node and antinode, cannot be determined. For an identical transmission spectrum there is more than one atom path due to the spatial symmetry of the cavity mode, and we call this the trajectory degeneracy. For example, for the usual TEM<sub>00</sub> mode, if we do not consider the cavity axis path, the left- and right-hand-side passing of the atom from the off axis causes the duplicate degeneracy of the atom trajectories, in principle. Higher-order transverse modes may break the spatial symmetry and reduce the degeneracy of the atom trajectories. In 2003, Puppe *et al.* demonstrated the single-atom trajectories in high-order transverse modes of a high-finesse optical cavity [23]. The atom trajectories were obtained according to the transmission spectrum of the cavity. However, the spatial patterns of TEM<sub>01</sub> and TEM<sub>10</sub> modes were oriented nearly horizontally and the atom trajectories were still duplicate degenerate. In this Rapid Communication, a tilted spatial transverse TEM<sub>10</sub> mode is used, which breaks the symmetry and allows complete elimination of the degeneracy of the atom trajectories. We use the strongly coupled atom-cavity system to track the atomic path and determine uniquely the ballistic trajectory of a single atom. A spatial resolution of  $5.6 \mu\text{m}$  is achieved in a time interval of  $10 \mu\text{s}$  along the vertical direction (axis  $x$ ), according to the statistical uncertainties based on the theoretical fittings, while the atom position along the horizontal direction (axis  $y$ ) can be obtained with a precision of  $0.1 \mu\text{m}$ . With the help of even higher-order modes and a smaller mode waist of the high-finesse cavity, it is capable of obtaining the trajectory of the single atom with a high spatial resolution by the so-called atomic kaleidoscope

<sup>\*</sup>Present address: School of Instrumentation Science and Opto-Electronics Engineering, BeiHang University, Beijing 100191, China.

<sup>†</sup>Corresponding author: tczhang@sxu.edu.cn

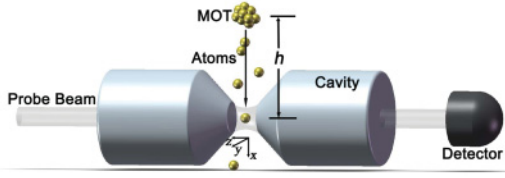


FIG. 1. (Color online) Experiment scheme. The atoms fall down freely from the magneto-optical trap (MOT) and pass through the higher transverse modes in the cavity. The optimum coupling constant  $g_0$  is larger than cavity decay rate  $\kappa$  and atom decay rate  $\gamma$ , so the interaction between the atom and cavity mode reaches the strong coupling regime.

[24,25] based on the atom-cavity microscope (ACM) system [14].

The CQED system contains a microcavity, and an atom couples to a single mode of the electromagnetic field as shown in Fig. 1. The interaction between the atom and the single-mode field is described by the oscillatory exchange of energy (Rabi oscillation), characterized by  $g$ . A real experimental system is an open system [26], and both the cavity decay rate  $\kappa$  and atom decay rate  $\gamma$  must be taken into account. In the strong coupling regimes the optimum coupling constant  $g_0$  in the TEM<sub>00</sub> mode is much larger than  $\kappa$  and  $\gamma$ .

A conventional magneto-optical trap (MOT) is positioned directly above the cavity. The atoms fall down and pass through the cavity due to gravity when the MOT is shut off. Without a trap inside the cavity, the single-atom trajectories of free-falling atoms into the cavity from above are straight lines, as is physically appropriate. The position of the atom along the cavity axis  $z$  plays an important role for the transmission spectrum. However, in the real experiments, since the cavity center is far from the MOT, the intracavity atom velocity in the horizontal direction is very small as compared to that in the vertical direction, and the motion along the cavity axis  $z$ , which is most likely caused by the force due to the weak probe beam, is small [14]. We thus assume that the atom trajectories in the cavity are vertical straight lines. Those transits corresponding to the transmissions dropping to nearly zero mean that the atoms pass through the antinode in a very narrow range in the cavity axis direction. The measured transmission spectra in the weak-field limit of a small excited state population is the 2D expression near the origin of the antinode ( $z \approx 0$ ):

$$T(x', y') = \left\{ [g_{\text{eff}}(x', y')^2 - \Delta_{pa}^2 + \Delta_{ca} \Delta_{pa} + \kappa \gamma]^2 + (\kappa \Delta_{pa} + \gamma \Delta_{pa} - \gamma \Delta_{ca})^2 \right\}^{-1} \kappa^2 (\gamma^2 + \Delta_{pa}^2). \quad (1)$$

Here  $\Delta_{pa} = \omega_{\text{probe}} - \omega_{\text{atom}}$  is the detuning between the probe light and atomic transition, and  $\Delta_{ca} = \omega_{\text{cavity}} - \omega_{\text{atom}}$  is the detuning between the cavity and the transition. The effective coupling  $g_{\text{eff}}$  for arbitrary Hermite-Gaussian transverse modes is dependent on the position of the atom in the cavity,  $g_{\text{eff}}(x', y') = g_0 \Psi_{m,n}(x', y') / \Psi_{0,0}(0, 0)$ . Here we have assumed the cavity axis is  $z$  and  $\Psi_{m,n}(x', y')$  are the mode functions of the cavity, expressed by

$$\Psi_{m,n}(x', y') = C_{m,n} \exp\left(-\frac{x'^2 + y'^2}{w_0^2}\right) H_m\left(\frac{\sqrt{2}x'}{w_0}\right) H_n\left(\frac{\sqrt{2}y'}{w_0}\right), \quad (2)$$

where  $C_{m,n} = (2^m 2^n m! n!)^{-1/2} (w_0^2 \pi / 2)^{-1/2}$ , and  $H_{m,n}$  are the corresponding Hermite polynomials of order  $m$  and  $n$ .  $w_0$  is the waist of the mode which is determined by the radius of curvature of mirrors and the cavity length. The transmission given by (1) is position dependent, thus the atomic trajectory may be determined from the spectrum of the cavity transmission. There is an angle of  $\theta = 45^\circ$  between the nodal lines of the TEM<sub>10</sub> modes and the  $x$  axis (the angle can be obtained experimentally), and a rotating coordinate transformation is thus used:  $x' = x \cos \theta - y \sin \theta$ ,  $y' = x \sin \theta + y \cos \theta$ .

Since the trajectories of the single atom are considered to be linear, according to expressions (1) and (2) with a rotating coordinate transformation, we can simulate the trajectories of the single atom. Figure 2 shows typical transmission spectra for a tilted TEM<sub>10</sub> mode with  $\Delta_{pa} = \Delta_{ca} = 0$ . Here we have used the parameters according to our experimental system:  $g_0 = 2\pi \times 23.9$  MHz,  $w_0 = 23.8$   $\mu\text{m}$ ,  $\gamma = 2\pi \times 2.6$  MHz, and  $\kappa = 2\pi \times 2.6$  MHz. From Fig. 2 we can see that the double-dip spectrum appears when the atom passed through the tilted TEM<sub>10</sub> mode due to the intensity distribution of two pieces separated by a nodal line. The double dip becomes more asymmetric as the atom trajectory is goes further from the center of the mode [ $y = \pm 10$   $\mu\text{m}$  and  $y = \pm 20$   $\mu\text{m}$ , shown in Figs. 2(a)–2(d) and 2(e)], while the transmission is symmetric with  $y = 0$ , as shown in Fig. 2(c). It is obvious that the cavity transmission is only dependent on the parameter  $y$ , and the trajectory of the single atom passing through the tilted TEM<sub>10</sub> mode thus can be determined uniquely.

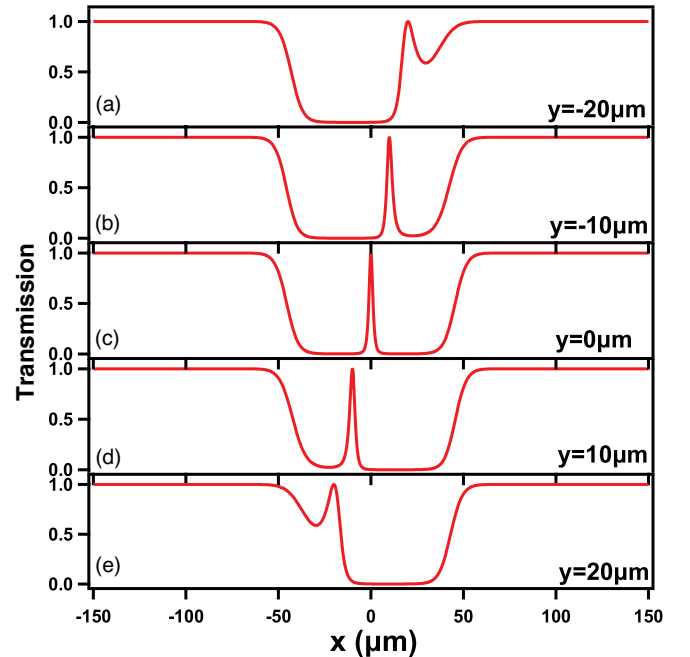


FIG. 2. (Color online) Cavity transmission spectra vs the atom's positions in the  $x$  axis for a TEM<sub>10</sub> mode for various off-axis distances  $y$  ( $y = 0, \pm 10$   $\mu\text{m}$ ,  $\pm 20$   $\mu\text{m}$ ) between the atoms' trajectories and the center of the mode. The detuning between the probe light and atom transition is  $\Delta_{ca} = 0$  MHz, and the detuning between the probe light and atom transition is also  $\Delta_{pa} = 0$  MHz.  $g_0 = 2\pi \times 23.9$  MHz,  $w_0 = 23.8$   $\mu\text{m}$ ,  $\gamma = 2\pi \times 2.6$  MHz, and  $\kappa = 2\pi \times 2.6$  MHz; all the parameters are used according to our experimental system.

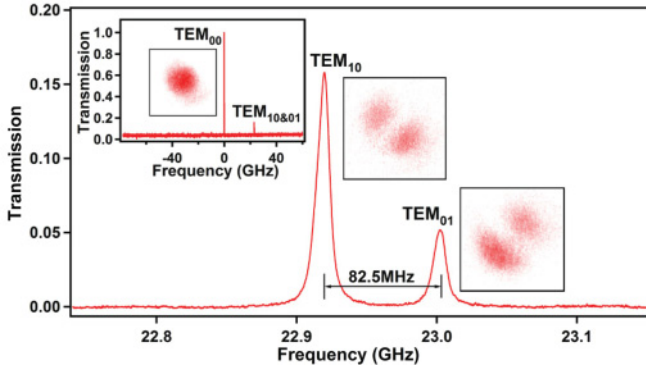


FIG. 3. (Color online) Cavity transmission vs the scanning of the probe frequency. The inset shows the  $TEM_{00}$ ,  $TEM_{10}$ , and  $TEM_{01}$  modes. Splitting  $\sim 82.5$  MHz between  $TEM_{10}$  and  $TEM_{01}$  mode is observed. Three images, from the left-hand side to the right-hand side, are the 2D intensity distributions of  $TEM_{00}$ ,  $TEM_{10}$ , and  $TEM_{01}$  modes directly detected by a CCD camera, respectively.

The experimental setup contains two important parts, including the cold atom cloud trapped by MOT [27] and the high-finesse Fabry-Pérot cavity composed of two spherical mirrors [28,29]. Both of them are located in an ultrahigh vacuum chamber. The MOT is located 5 mm above the cavity with an atom number of  $\sim 10^5$ . The length of the cavity is  $86 \mu\text{m}$  with a waist of the  $TEM_{00}$  mode of  $w_0 = 23.8 \mu\text{m}$ . The finesse of cavity is  $F = 330\,000$  and the parameters of the system are  $(g_{10}, \kappa, \gamma) = 2\pi \times (20.5, 2.6, 2.6)$  MHz, where  $g_{10}$  is the coupling coefficient of an atom at the position of maximum coupling in either of the two lobes of the  $TEM_{10}$  mode. The intracavity mean photon number is  $m \approx 1$ . The cavity is locked to the cesium  $D2$  transition  $6^2S_{1/2}$ ,  $F = 4 \rightarrow 6^2P_{3/2}$ ,  $F' = 5$ . Single-photon counting modules (SPCMs) [30] are used to detect the cavity transmission. Figure 3 shows the cavity transmission versus the scanning of the frequency of the probe light. The inset in Fig. 3 shows the  $TEM_{00}$ ,  $TEM_{10}$ , and  $TEM_{01}$  modes, respectively. In an ideal case the transverse modes with the same  $m + n$  should be degenerate, but the real cavity in the experiment gives a splitting  $\sim 82.5$  MHz between the  $TEM_{10}$  and  $TEM_{01}$  modes, which is due to the geometric imperfection of the mirrors [28,29]. The corresponding 2D distributions of the intensities of the modes are also obtained by a charge-coupled device (CCD) camera, and the patterns of the modes help us to determine directly the angle between the nodal lines of the  $TEM_{10}$  and  $TEM_{01}$  modes and the  $x$  axis, which is  $\sim 45^\circ$  by chance.

The cavity transmission spectra versus time with a single atom passing through the cavity  $TEM_{10}$  mode are shown in Fig. 4. Here the probe is resonant to the cavity. The red dots are the experimental data and the green solid curves are the theoretical fittings according to expression (1). It is clear from Fig. 4 that different double peaks of the transmission spectra are observed, depending on the position of the atoms. The two dips are symmetrical when the atom trajectory is located at  $y = 0 \pm 0.2 \mu\text{m}$  [see Figs. 4(b) and 4(e)]. The fitted atom velocity is  $0.39 \pm 0.01$  m/s. When the atom trajectory is not at  $y = 0$ , that is, for  $y < 0$  or  $y > 0$ , the two dips are asymmetrical. For  $y < 0$ , the former dip is deeper and wider, and it is just the reverse for  $y > 0$ . Thus the atom trajectory degeneracy is eliminated. Figures 4(a) and 4(c) show the transmission

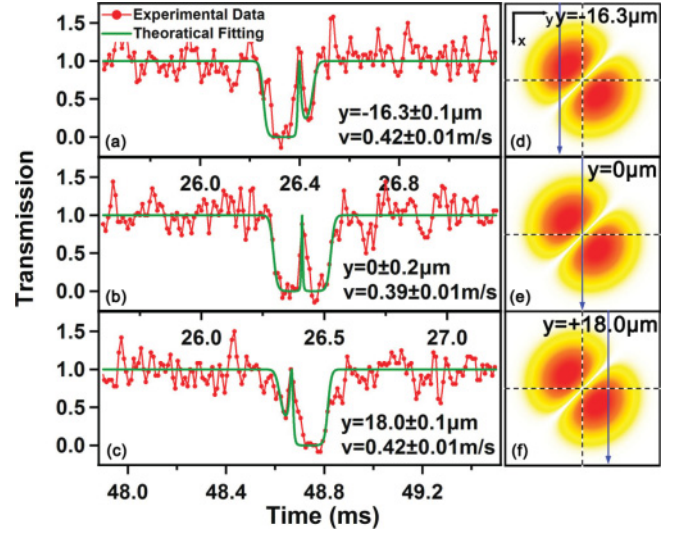


FIG. 4. (Color online) The cavity transmission spectra of a single atom coupled to the tilted  $TEM_{10}$  mode of a high-finesse optical cavity. The red dots are the experimental data and the green solid curves are theoretical fitting according to expression (1). (a)  $y = -16.3 \pm 0.1 \mu\text{m}$ ,  $v = 0.39 \pm 0.01$  m/s. (b)  $y = 0 \pm 0.2 \mu\text{m}$ ,  $v = 0.42 \pm 0.01$  m/s. (c)  $y = 18.0 \pm 0.1 \mu\text{m}$ ,  $v = 0.42 \pm 0.01$  m/s. The right-hand side figures (d), (e), and (f) show the unique atom trajectories corresponding to (a), (b), and (c), respectively.  $\Delta_{pa} = 0$  MHz. ( $g_0 = 2\pi \times 23.9$  MHz,  $w_0 = 23.8 \mu\text{m}$ ,  $\gamma = 2\pi \times 2.6$  MHz and  $\kappa = 2\pi \times 2.6$  MHz.)

spectra corresponding to  $y = -16.3 \mu\text{m} \pm 0.1 \mu\text{m}$  and  $y = +18.0 \mu\text{m} \pm 0.1 \mu\text{m}$ , a left-hand side transit and a right-hand side transit, respectively. The spatial resolution in the vertical direction (axis  $x$ ) is  $\sim 5.6 \mu\text{m}$  in a  $10\text{-}\mu\text{s}$  time interval while it is  $0.1 \mu\text{m}$  for the off axis ( $y$  direction). The resolution is determined by the statistical uncertainties based on the theoretical fittings. The resolution for the off axis is much better than the resolution for the vertical direction, and it is also much better than the reported result in Hood's experiment [14]; this is simply due to the break of the spatial symmetry of the tilted  $TEM_{10}$  mode and the depth of the two transmission dips that allows such a measurement with good resolution in the  $y$  direction. The atom velocity is  $0.42 \pm 0.01$  m/s. We have observed diverse transmission spectrums. If  $y < 0$ , the atom passes through the upper part of the  $TEM_{10}$  mode first and then passes through the lower part [see Fig. 4(d)], and vice versa [see Fig. 4(f)]. Both the atom trajectory and atom velocity are uniquely determined with this tilted higher-order transverse mode in the high-finesse cavity. The precision is mainly limited by the horizontal movement during the transit process caused by the probe light and the uncertainty from the fluctuation of the Poisson photon-counting statistics. Of course, here we still have one fundamental ambiguity: We do not know the specific antinode in which the atom passes through.

It should be mentioned that for a small fraction of atom transits, corresponding to those atoms passing away from the antinode and very close to the node of the cavity mode, the method of determining the off-axis  $y$  cannot be applied. For these atom transits, the transmission cannot drop to the bottom, and the trajectory determination fails in this case due to the poor signal-to-noise ratio. However, in the relatively

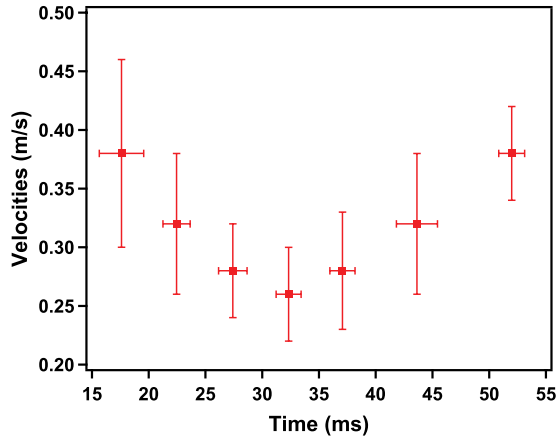


FIG. 5. (Color online) The velocities of atoms at the cavity at different arrival times. The result is obtained from 200 times of atom transits based on the strong coupling between atoms and the cavity mode.

wide range of  $z = -150$  nm to  $+150$  nm, the transmission drops down to almost zero. From the recorded transits there are  $\sim 60\%$  in this range.

Figure 5 plots the independently determined flight time against velocity, which is obtained from 200 times of atom transits based on this strong coupling system. We have directly measured a large number of atom velocities passing through the cavity mode and obtain the temperature of the atom cloud according to the statistical results. We find that there exists a minimum velocity at the arrival time of  $\sim 32$  ms, which corresponds to the time interval of an atom with zero velocity that falls down freely in 5 mm and is coincident with the experiment. Those earlier and later arrived atoms with nonzero

velocities, corresponding to downward and upward movement initially, have higher velocities. We thus observed a V-shape distribution of the velocity of the atoms, and this velocity distribution is also coincident with the results in Fig. 4. This gives the temperature of the atoms in the MOT,  $186 \mu\text{K} \pm 19 \mu\text{K}$ .

In summary, we have investigated the trajectories and velocities of single neutral cesium atoms coupled to a tilted  $\text{TEM}_{10}$  mode in a high-finesse optical cavity. The degenerate trajectory of a single atom is eliminated completely due to the break of the geometry of the spatial mode in the cavity. The unique track of the single atom is determined. The velocity of the atoms is also measured. The transmission spectra are fitted very well in the weak-field approximation of the strong coupling between a tilted  $\text{TEM}_{10}$  Hermite-Gaussian transverse mode and an atom. We yield  $5.6 \mu\text{m}$  of spatial resolution in a  $10\text{-}\mu\text{s}$  time interval along the vertical direction (axis  $x$ ) and  $0.1 \mu\text{m}$  for the off axis ( $y$  direction). The high resolution in the off-axis direction is a result of the symmetry breaking of the tilted intra-cavity  $\text{TEM}_{10}$  mode. The unique determination of the single atom trajectory is impossible for the usual  $\text{TEM}_{00}$  mode. This method can be extended to sense the atomic center-of-mass motion and the kinetic energy of a single atom in real time, with better spatial and time resolutions when the higher transverse modes and smaller mode volumes are used to confine and cool the atoms three dimensionally in an optical cavity; this may develop the time-resolved microscopy based on the strong coupling atom-cavity microscope [14,31,32].

The work is supported by the National Nature Science Foundation of China (Project No. 10794125, 60808006, 60821004, 61078051, 60978017 and the 973 program).

- 
- [1] N. Schlosser *et al.*, *Nature (London)* **411**, 1024 (2001).
  - [2] J. Beugnon *et al.*, *Nature (London)* **440**, 779 (2006).
  - [3] D. Frese *et al.*, *Phys. Rev. Lett.* **85**, 3777 (2000).
  - [4] D. Schrader *et al.*, *Phys. Rev. Lett.* **93**, 150501 (2004).
  - [5] M. K. Tey *et al.*, *Nat. Phys.* **4**, 924 (2008).
  - [6] L. Slodicka, G. Hetet, S. Gerber, M. Hennrich, and R. Blatt, *Phys. Rev. Lett.* **105**, 153604 (2010).
  - [7] J. Ye, D. W. Vernooy, and H. J. Kimble, *Phys. Rev. Lett.* **83**, 4987 (1999).
  - [8] J. McKeever *et al.*, *Science* **303**, 1992 (2004).
  - [9] A. Kubanek *et al.*, *Nature (London)* **462**, 898 (2009).
  - [10] M. Koch *et al.*, *Phys. Rev. Lett.* **105**, 173003 (2010).
  - [11] M. Mücke *et al.*, *Nature (London)* **465**, 755 (2010).
  - [12] S. Parkins, *Nature (London)* **465**, 699 (2010).
  - [13] M. L. Terraciano *et al.*, *Nat. Phys.* **5**, 480 (2009).
  - [14] C. J. Hood *et al.*, *Science* **287**, 1447 (2000).
  - [15] H. Mabuchi *et al.*, *Opt. Lett.* **21**, 1393 (1996).
  - [16] P. Munstermann *et al.*, *Opt. Commun.* **159**, 63 (1999).
  - [17] T. P. Purdy *et al.*, *Phys. Rev. Lett.* **105**, 133602 (2010).
  - [18] M. G. Raizen, R. J. Thompson, R. J. Brecha, H. J. Kimble, and H. J. Carmichael, *Phys. Rev. Lett.* **63**, 240 (1989).
  - [19] G. Rempe, R. J. Thompson, R. J. Brecha, W. D. Lee, and H. J. Kimble, *Phys. Rev. Lett.* **67**, 1727 (1991).
  - [20] R. J. Thompson, G. Rempe, and H. J. Kimble, *Phys. Rev. Lett.* **68**, 1132 (1992).
  - [21] E. L. Raab, M. Prentiss, Alex Cable, Steven Chu, and D. E. Pritchard, *Phys. Rev. Lett.* **59**, 2631 (1987).
  - [22] J. D. Miller, R. A. Cline, and D. J. Heinzen, *Phys. Rev. A* **47**, R4567 (1993).
  - [23] T. Puppe, P. Maunz, T. Fischer, P. W. H. Pinkse, and G. Rempe, *Phys. Scr. T* **112**, 7 (2004).
  - [24] P. Maunz *et al.*, *Opt. Lett.* **28**, 46 (2003).
  - [25] P. Horak *et al.*, *Phys. Rev. Lett.* **88**, 043601 (2002).
  - [26] H. J. Carmichael, *An Open Systems Approach to Quantum Optics* (Springer, Berlin, 1993).
  - [27] P. Zhang *et al.*, *Phys. Rev. A* **80**, 053420 (2009).
  - [28] G. Li *et al.*, *Appl. Opt.* **45**, 7628 (2006).
  - [29] C. J. Hood, H. J. Kimble, and J. Ye, *Phys. Rev. A* **64**, 033804 (2001).
  - [30] Y. Li *et al.*, *Phys. Rev. A* **76**, 013829 (2007).
  - [31] H. Mabuchi, J. Ye, and H. J. Kimble, *Appl. Phys. B* **68**, 1095 (1999).
  - [32] Z. Q. Yin, T. C. Li, and M. Feng, *Phys. Rev. A* **83**, 013816 (2011).